# Crosslinking of DNA repair and replication proteins to DNA in cells treated with 6-thioguanine and UVA

## Quentin Gueranger, Azadeh Kia, David Frith and Peter Karran*

Cancer Research UK London Research Institute, Clare Hall Laboratories, South Mimms, EN6 3LD, UK

## ABSTRACT

**The DNA of patients taking immunosuppressive and anti-inflammatory thiopurines contains 6-thioguanine (6-TG) and their skin is hypersensitive to ultraviolet A (UVA) radiation. DNA 6-TG absorbs UVA and generates reactive oxygen species that damage DNA and proteins. Here, we show that the DNA damage includes covalent DNA–protein crosslinks. An oligonucleotide containing a single 6-TG is photochemically crosslinked to cysteine-containing oligopeptides by low doses of UVA. Crosslinking is significantly more efficient if guanine sulphonate ($G^{SO3}$)—an oxidized 6-TG and a previously identified UVA photoproduct—replaces 6-TG, suggesting that $G^{SO3}$ is an important reaction intermediate. Crosslinking occurs via oligopeptide sulphydryl and free amino groups. The oligonucleotide–oligopeptide adducts are heat stable but are partially reversed by reducing treatments. UVA irradiation of human cells containing DNA 6-TG induces extensive heat- and reducing agent-resistant covalent DNA–protein crosslinks and diminishes the recovery of some DNA repair and replication proteins from nuclear extracts. DNA–protein crosslinked material has an altered buoyant density and can be purified by banding in cesium chloride (CsCl) gradients. PCNA, the MSH2 mismatch repair protein and the XPA nucleotide excision repair (NER) factor are among the proteins detectable in the DNA-crosslinked material. These findings suggest that the 6-TG/UVA combination might compromise DNA repair by sequestering essential proteins.**

## INTRODUCTION

Since their development >50 years ago, thiopurine pro-drugs have been widely used as immunosuppressants and in cancer therapy. They are now increasingly prescribed in the treatment of chronic relapsing inflammatory disorders such as inflammatory bowel disease. Azathioprine, the most extensively prescribed immunosuppressant in organ transplant patients, is classed as a human carcinogen by IARC (1). This designation reflects the 100- to 200-fold increased incidence of skin cancer that accompanies long-term azathioprine use following organ transplantation (2,3). Although epidemiological evidence implicates both the duration of immunosuppression and sunshine exposure in this hugely increased cancer risk, the way that these factors interact in the development of skin cancer remains unclear.

The end products of thiopurine metabolism, 6-thioguanine (6-TG) nucleotides, are substrates for incorporation into nucleic acids and the DNA of azathioprine patients accumulates measurable amounts of 6-TG (4–6). Unlike the canonical DNA bases, 6-TG absorbs ultraviolet A (UVA) and DNA 6-TG is photochemically activated by wavelengths around 340 nm to generate singlet oxygen ($^1O_2$) (7), a form of reactive oxygen species (ROS) that can damage both DNA and proteins (6,8). UVA comprises >90% of the ultraviolet radiation in incident sunlight and the skin of patients receiving azathioprine is hypersensitive to simulated sunlight and to UVA, but not to UVB (6,9). This UVA hypersensitivity is consistent with the formation of DNA photodamage in skin although the nature of this damage remains incompletely defined. To obtain a better understanding of the UVA sensitivity of DNA in azathioprine patients and whether photochemical DNA lesions might contribute to their skin cancer risk, we are investigating photochemical reactions of DNA 6-TG.

Work in model cell culture systems has established that $^1O_2$ generated from DNA 6-TG is hazardous. Low doses of UVA are mutagenic and extremely toxic to cells containing DNA 6-TG (6). At the molecular level, the low oxidation potential of DNA 6-TG makes it a preferred target and DNA-generated ROS cause its rapid oxidation to guanine sulphinate ($G^{SO2}$) and guanine sulphonate ($G^{SO3}$) (10). Both these DNA 6-TG oxidation products are potent blocks to replication and transcription *in vitro* (7,11). The vulnerability of DNA containing 6-TG is

*To whom correspondence should be addressed. Tel: 020 7269 3870; Fax: 020 7269 3812; Email: peter.karran@cancer.org.uk

further emphasized by its susceptibility to breakage—both single and double strand—by low doses of UVA. S-phase cells are particularly vulnerable, in this regard, and some or all of the 6-TG/UVA induced DNA lesions trigger DNA damage responses and associated cell cycle checkpoints (12).

ROS generated from DNA 6-TG also damage proteins. $^1O_2$ targets the histidine and aromatic residues of proteins (13,14). Consistent with these reaction preferences, subunits of the Proliferating cell nuclear antigen (PCNA) replication processivity factor become covalently crosslinked via histidine in cells treated with 6-TG and UVA (6,8). This efficient PCNA crosslinking suggested that DNA-associated proteins might be particularly susceptible to photochemical damage involving DNA 6-TG. PCNA clamps replication factors to DNA by encircling the DNA helix. Many DNA processing proteins, including RNA polymerase II (15,16) and the mismatch recognition factor MutSα (17), employ similar strategies. The particularly intimate DNA–protein contact involved in these interactions might render these proteins exceptionally vulnerable to DNA-generated ROS. Here, we demonstrate that DNA 6-TG interacts with UVA to cause rapid covalent attachment of proteins to DNA. This is observed *in vitro* in reactions between oligopeptides and 6-TG containing oligonucleotides and *in vivo* as the covalent attachment of nuclear proteins to DNA of UVA irradiated cultured cells. DNA repair and replication factors are identified among the crosslinked proteins. This raises the possibility that these processes may be compromised by photochemical reactions of DNA 6-TG.

## MATERIALS AND METHODS

### Cell culture and chemicals

Human mismatch-repair deficient (MLH1) defective (18) CCRF-CEM leukaemia cells were grown in RPMI, supplemented with 10% fetal calf serum. Chemicals were purchased from Sigma-Aldrich (St Louis, MO, USA) unless otherwise stated. Cells were radiolabelled by overnight incubation with 2-[$^{14}$C]-thymidine at 0.1 μCi/ml (Perkin Elmer, Waltham, MA, USA). UVA irradiations were performed as described before (8).

### 2D-DIGE

Materials, apparatus and software were all from GE Healthcare (Piscataway, NJ, USA). Quadruplicate independent nuclear extracts (50 μg protein) of cells that had received the same 6-TG/UVA treatment were labelled with 0.4 pmol Cy3/Cy5 CyDye. For the first dimension, 150 μg of CyDye labelled proteins were cuploaded onto rehydrated IEF pH 3-7 NL Immobiline DryStrip strips. Isoelectric focusing was performed on an Ettan IPGphor IEF system using the Ettan IPGphor cup loading manifold. Following IEF, the second dimension separation was carried out on 12% polyacrylamide gels. Fluorescently labelled proteins were visualized using a Typhoon 9400 variable mode imager and Typhoon scanner control software, version 3.0. All images were cropped using ImageQuant tools to exclude non-essential

information prior to DeCyder analysis. Analysis of gel images was performed using DeCyder differential analysis software version 6.5. Protein spots with a 1.5-fold difference in abundance and a Student's *t*-test value of $P \leq 0.01$ were selected. Preparative gels for spot picking were stained using 0.1% colloidal coomassie blue G-250 (Sigma Aldrich) for 4 days. Protein spots of interest were manually excised from the stained gels.

### Mass spectrometry

Peptides for analysis were generated by *in situ* tryptic digestion of protein/gel bands. LC-MS/MS analysis of the peptides was carried out on a LTQ Orbitrap XL/ETD mass spectrometer (ThermoScientific, Waltham, MA, USA) and the data searched against a concatenated, non-redundant protein database (UniProt KB15.5), using the Mascot search engine (Matrix Science, London, UK).
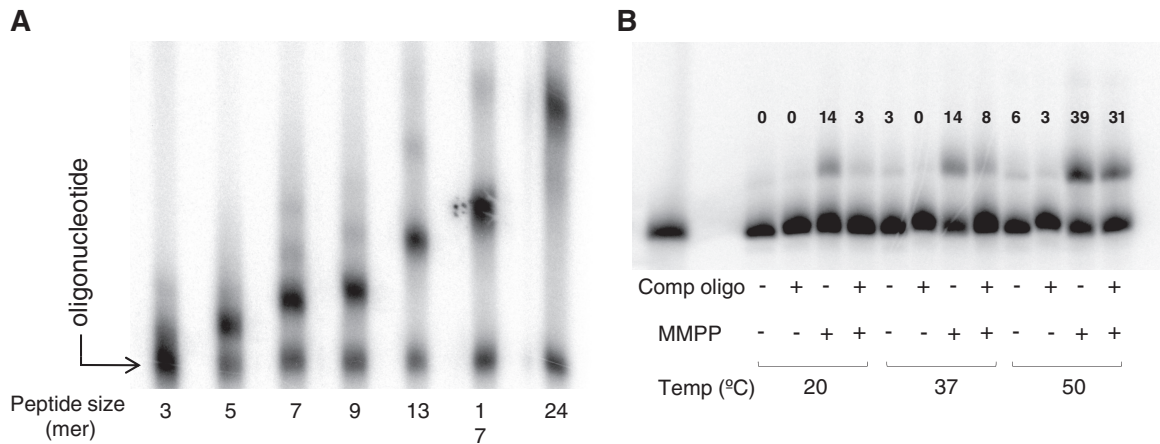
### Genomic DNA preparation

Cells were treated for 48 h with 0.8 μM 6-TG in complete medium. After irradiation, they were transferred to Eppendorf tubes and lysed by addition of three pellet volumes of Buffer 1 (10 mM Tris–HCl pH 7.4, 2.5 mM $MgCl_2$, 0.5% NP40, 1 mM DTT) containing protease inhibitors (Roche, Basel, Switzerland). After 10 min on ice, the sample was centrifuged at 10 000 rpm for 10 min and the pellet was re-suspended in 3 pellet volumes of Buffer 2 (25 mM sodium phosphate pH 7.4, 0.5 M NaCl, 1 mM EDTA, 0.5% Triton X-100, 10% Glycerol, 5 mM $MgCl_2$, 1 mM DTT) containing protease inhibitors. After a further 30 min on ice, the sample was centrifuged for 20 min and the supernatant (the soluble chromatin fraction) was retained. The pellet was washed twice in Buffer 2 and finally resuspended in 400 μl of the same buffer. The sample (containing DNA and associated proteins) was extensively sheared by passage 20 times through a 19-gauge needle, then a 21-gauge and finally through a 23-gauge needle.

### Isopycnic cesium chloride gradient analysis

The sheared DNA sample (100 μg) was mixed with 13 ml of cesium chloride (CsCl) solution in TE (starting density of 1.4, unless indicated) and centrifuged at 60 000 rpm for 16 h at 4°C in a Beckman Vti70.1 fixed angle rotor. Fractions were collected from the bottom of the tube. $A^{260nm}$ was determined by Nanodrop 2000 (Thermo scientific) and $^{14}$C content by scintillation counting.

In experiments in which gradient fractions were probed by immunoblotting, cell extracts were prepared in RIPA buffer and sonicated (Branson sonifier: 20 times 0.5 s pulses at 15% power) before DNA banding on CsCl gradients. Appropriate gradient fractions were pooled and desalted on PD-10 columns (GE Healthcare Piscataway, NJ, USA) equilibrated in water. Aliquots were applied to a N$^+$ hybond membrane and crosslinked with UVC. The membranes were probed with antibodies against PCNA (PC10: Santa Cruz, Santa Cruz, CA, USA), XPA (Clone 12F5: Abcam, Cambridge, MA, USA), MSH2 (Clone FE11: Oncogene) CASPASE 5-p20

(Clone D18: Santa Cruz) MCM2 (A300-191A: Bethyl, Montgomery, TX, USA). Goat and mouse HRP secondary antibodies were from Biorad (Hercules, CA, USA).

### *In vitro* crosslinking

The 26-mer oligonucleotide (5′-CGATCTGATGTXAGA GCAGACAGCAG-3′ where X = 6-thio 2′-deoxyguanine) was purchased from Oligos Etc. (Wilsonville, OR, USA). When required, the complementary strand in which C was placed opposite 6-TG was annealed. For oxidation, 1 nmol was treated with 1 μmol of magnesium monoperoxyphthalate (MMPP) for 30 min at RT followed by ethanol precipitation and extensive washing. The oxidized oligonucloetide was incubated with 150 nmol oligopeptide for 16 h at 50°C in 50 mM Tris pH 7.5. The oligopeptides, all of which contained a single cysteine, were synthesized by the in-house CR-UK LRI facility. Their sequences were as follows:

24-mer: AEIDEDKCIGCGACAEACPTGAIE; 17-mer: PGNGQTAECGATQGNGP; 13-mer: NGQTA ECGATQGN; 9-mer: QTAECGATQ; 7-mer TAECG AT; 5-mer: AECGA. Reaction products were separated on a 16% sequencing gel, excised, extracted and purified by precipitation.

## RESULTS

### DNA–peptide crosslinks *in vitro*

Previous work (10) established that UVA photoactivated 6-TG forms addition products with low molecular weight thiol compounds. To investigate whether protein thiols are similarly vulnerable to photochemical crosslinking to DNA, we first examined the reactions between a synthetic oligonucleotide and oligopeptides. In initial experiments, a single-stranded 26-mer oligonucleotide containing 6-TG was UVA irradiated and incubated with a 7-mer TAECGAT oligopeptide that contained a single cysteine. Following overnight incubation at 50°C, a UVA- and peptide-dependent formation of slowly

migrating products was revealed by denaturing PAGE analysis (Figure 1A). At 50 kJ/m$^2$ UVA, this product accounted for ~10% (average of three experiments; range = 9.3–12.6%) of the input oligonucleotide. Pre-treatment of the oligonucleotide with MMPP to quantitatively convert the 6-TG to G$^{SO3}$, significantly improved the reaction efficiency and under the same reaction conditions 30–50% of the input oligonucleotide was converted to the slowly migrating form (Figure 1B). These observations are consistent with G$^{SO3}$, which is a relatively minor UVA photoproduct but is produced quantitatively by MMPP treatment, being a likely reaction intermediate.

Similar addition reactions occurred with longer oligopeptides. Peptides up to 24-mer, each containing a single cysteine, were efficiently (~50%) crosslinked to an oxidized 6-TG oligonucleotide during overnight incubation at 65°C (Figure 2A). Product yield was increased to ~80% by incubation at 80°C.

Double-stranded 6-TG containing DNA was around 4-fold less reactive than ssDNA at 20°C, and 1.3-fold less reactive at 50°C, indicating that secondary structural elements significantly influence the crosslinking reaction (Figure 2B).

### DNA 6-TG crosslinking via peptide thiol and amino groups

In the majority of products, the 7-mer oligopeptide (TAECGAT) was crosslinked to the oligonucleotide through its single cysteine. When serine (S) replaced cysteine (C), product formation was reduced by ≥50% (Figure 3A, lanes 1 and 2) but not abolished. Residual crosslinking to the TAESGAT oligopeptide was completely eliminated by acetylation (Ac) of the N-terminal amino group (lane 3). A similar N-terminal block reduced crosslinking to TAECGAT by about one-third (lane 4). These findings, which are quantified in Supplementary Figure S1, suggested the formation of both S-bonded (via cysteine) and N-bonded (via the free N-terminal NH$_2$ group) peptide–DNA products. This possibility was



**Figure 1.** Crosslinking of a 7-mer TAECGAT peptide to a 26-mer oligonucleotide. (**A**) 6-TG-containing oligonucleotide was irradiated with the indicated doses of UVA or oxidized with MMPP before incubation at 50°C with (+) or without (−) the oligopeptide. After 16 h, the reaction products were resolved by PAGE. Asterisks indicate the major crosslinked species. A minor product is also indicated double asterisks. (**B**) The efficiency of oligonucleotide crosslinking by UVA- and MMPP-treated oligonucleotides. Data from three independent experiments as described in A were quantified by ImageQuant analysis. Mean values are shown and error bars represent the range of values.

**Figure 2.** Crosslinking of different peptides to a 6-TG containing oligonucleotide. (**A**) The 6-TG oligonucleotide was oxidized by MMPP and incubated for 16 h at 65°C with oligopeptides of the length indicated all of which contained a single cysteine. Reaction products were resolved by PAGE. (**B**) The MMPP-oxidized 26-mer oligonucleotide was annealed to its complementary (comp) strand as shown and incubated with the 7-mer peptide for 16 h at the indicated temperatures. Products were resolved by PAGE. The percentage of crosslinked oligonucleotide indicated at the top of each lane. The sample in the far left lane is 26-mer oligonucleotide that had been incubated at 50°C in the absence of oligopeptide.
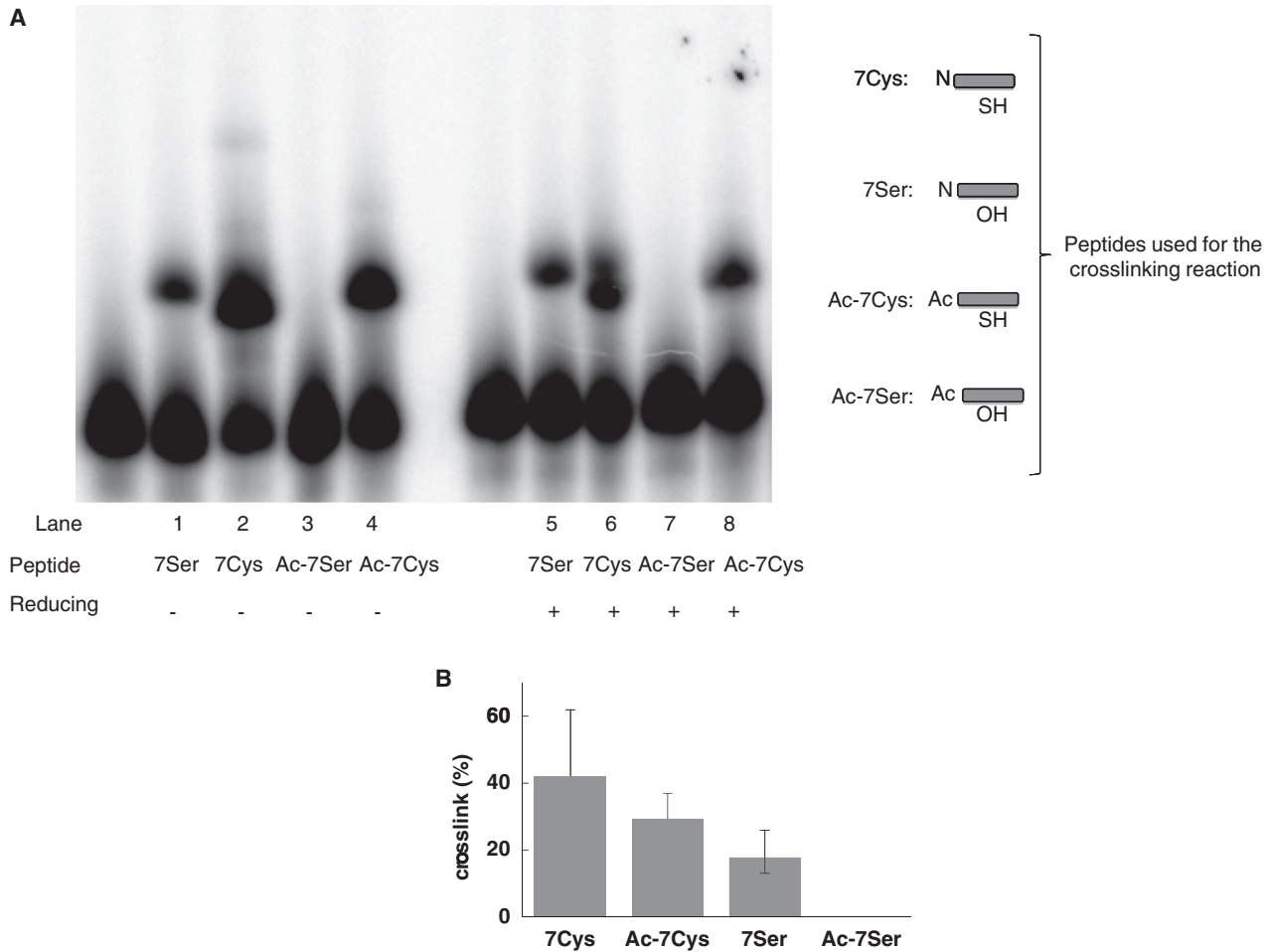


**Figure 3.** Functional groups involved in crosslinking. (**A**) MMPP-oxidized 26-mer 6-TG-containing oligo was incubated with 7-mer peptides. Containing either cysteine (Cys) or serine (Ser). Where indicated, the terminal $NH_2$ group was acetylated (Ac). The peptides are shown schematically to the right of the gel image. The cysteine thiol (SH) and the serine OH groups are shown. The reaction was allowed to continue for 16 h at 65°C and products resolved by PAGE. The products in lanes 5–8 were treated with reducing agents (100 mM DTT, 10% β-mercaptoethanol) for 15 min at 95°C before loading. (**B**) Average crosslinking efficiencies, based on at least three experiments. Error bars represent range of values.

investigated further by treating the crosslinked species with reducing agents. Figure 3A (right panel) shows that the products formed with TAESGAT were impervious to reducing treatment (lane 5) whereas the same treatment abolished around two-thirds of crosslinks formed by TAE**C**GAT (lane 6) or its N-terminally blocked counterpart (lane 8). In addition to the major crosslinked species with TAE**C**GAT, we consistently noted a more slowly migrating species that accounted for 3–5% of the total (lane 2). This product was also reversed by reducing treatment, compatible with an S–S linkage and was not formed with TAESGAT. These findings indicate that peptides can become either S-bonded or N-bonded to DNA containing 6-TG. The proposed structures of the different products are also shown schematically in Supplementary Figure S1.

## Crosslinking *in vivo*: 2D-DIGE analysis of nuclear proteins

The efficient crosslinking of peptides to 6-TG-containing oligonucleotides suggested that covalent attachment of protein to DNA 6-TG might occur frequently in UVA-treated cells. This possibility was examined by 2D-DIGE. Briefly, CCRF-CEM cells were allowed to incorporate 6-TG for 48 h and then irradiated with $10 \, kJ/m^2$ UVA. Control cells received 6-TG but were unirradiated. Nuclear proteins were prepared and derivatized with fluorescent chromophores. Extracts from irradiated and unirradiated cells were mixed and analysed by 2D gel electrophoresis. DeCyder 2D software was used to identify proteins present at significantly altered levels in irradiated cell extracts (a representative gel is shown in Supplementary Figure S2). Individual proteins were excised from a separate coomassie-stained gel and identified by mass spectrometry. Two examples of the analysis are shown in Figure 4 and Table 1 summarizes the nuclear proteins that were reproducibly altered by the treatment. PCNA provides an internal validation since we have previously demonstrated that its subunits become photochemically crosslinked.

## Reduced levels of nuclear mismatch repair proteins after 6-TG + UVA treatment

Since the 2-D DIGE screen identified MSH2, we examined the effect of 6-TG/UVA on the levels of MSH2 and its partner protein MSH6 by western blotting. Figure 5A shows that the recovery from UVA irradiated CCRF-CEM cells of soluble nuclear MSH2 decreases in a UVA dose-dependent manner. Parallel experiments indicated that the reduced recovery was also 6-TG dose dependent (data not shown). When the post-Triton DNA fraction (which contains tightly bound proteins) was sonicated and analysed by western blotting, material reacting with the MSH2 antibody was detected as a high molecular weight smear (Figure 5B). Only a small fraction was present at the expected size of monomeric MSH2. This suggested that a significant fraction of MSH2 was in the form of high-molecular weight complexes that were not reversed by the reducing treatment used in sample preparation.
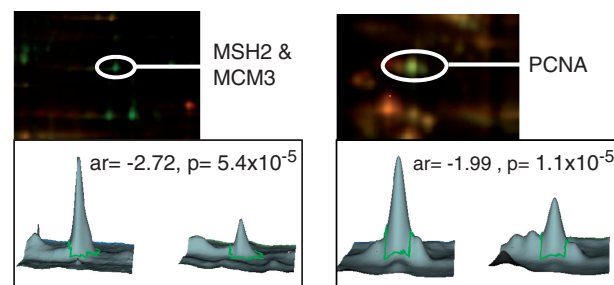


**Figure 4.** Examples of proteins with reduced representation on 2-D gels. Cropped sections of a representative 2D DIGE gel. 6-TG (green) and 6-TG + UVA (red)-treated samples were analysed on a 12% gel following a pH 3–7 NL isoelectric focusing. Values indicated correspond to the expression difference (ar) and the *P*-value, based on *t*-tests. Protein representation was quantified using DeCyder 2D software v6.5 (Lower panels).

**Table 1.** Nuclear proteins with significantly altered expression in 6-TG + UVA-treated cells

|  | Average ratio | *t*-test |
|---|---|---|
| **Down-regulated** | | |
| DNA damage binding protein 1 | −2.11 | 1.50E-03 |
| MSH2[a] | −2.72 | 5.40E-05 |
| ATP-dependant helicase 2 | −2.68 | 1.50E-04 |
| MCM 6 | −2.36 | 8.30E-05 |
| MCM 7 | −2.25 | 1.30E-05 |
| PCNA | −1.99 | 1.10E-05 |
| High-mobility protein group 1 | −3.48 | 4.00E-03 |
| Programmed cell death 6 | −1.62 | 1.10E-03 |
| PARK7 | −1.55 | 1.60E-03 |
| Glutathione transferase omega | −1.66 | 2.60E-03 |
| Heterogeneous nuclear ribonucleoprotein H | −1.53 | 1.00E-02 |
| Histone binding protein RBBP4 | −2.05 | 1.80E-04 |
| Ubiquitin activating Enzyme UBA2 | −4.83 | 1.80E-05 |
| **Up-regulated** | | |
| Prohibitin | +2.31 | 3.10E-04 |

[a]MCM3 peptides were also detected in the picked spot but did not contribute significantly (4 peptides, 5% protein coverage as opposed to 17 peptides, 20% coverage). Criteria for inclusion were: Nuclear localization. Consistent change in abundance of ≥1.5-fold. *T*-test: *P*-value ≤$10^{-2}$

Combined 6-TG and UVA treatment also affected the recovery of MSH6, the partner of MSH2 in the MutSα mismatch recognition heterodimer. Supplementary Figure S3 shows that the amount of MSH6 recovered from the triton-soluble fraction decreased in a 6-TG dose-dependent manner and that this was dependent on UVA. A similar analysis indicated that MSH6 was also present in the high-molecular weight DNA-containing material. Recovery of MSH2 and MSH6 from the cytoplasmic fraction was not detectably affected by 6-TG/UVA treatment (data not shown).

## 6-TG and UVA induce DNA–protein crosslinks in genomic DNA

Isopycnic density gradient analysis was used to investigate possible covalent photochemical crosslinking of nuclear proteins to DNA. CCRF-CEM cells containing DNA
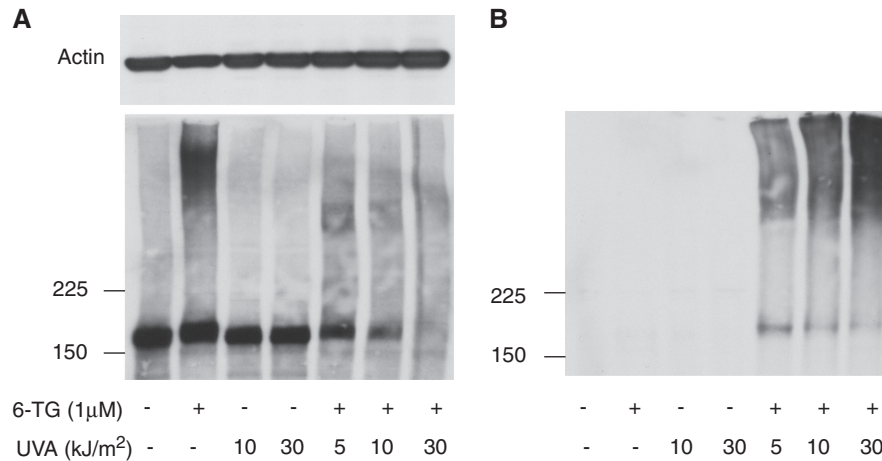
**Figure 5.** 6-TG/UVA-dependent decreased recovery of nuclear MSH2. CCRF-CEM cells were treated for 48 h with 6-TG and irradiated with UVA as indicated. Triton-soluble (**A**) and sonicated triton-insoluble fractions (**B**) were analysed by western blotting using an anti-MSH2 antibody.

labelled with 2-[14C]-thymidine and 6-TG were UVA irradiated. Native dsDNA and proteins have buoyant densities of ≥1.7 and ≤1.3, respectively (19). This difference allows their clear separation on CsCl gradients. Following cell fractionation by sequential treatments with detergent-based extraction buffers, DNA was recovered and the DNA solution adjusted to a density of 1.7 with CsCl. Gradients were centrifuged to equilibrium, fractionated and DNA quantified by scintillation counting. Under these conditions, the amount of DNA banding in the middle of the gradient corresponding to the position of native, double stranded DNA (density approximately 1.7) declined in a UVA and 6-TG-dependent fashion. An increasing proportion of the input radioactivity was recovered in low buoyant density fractions that also contained protein (data not shown). In subsequent experiments, the starting density of the gradients was adjusted to 1.40, to monitor a possible shift in DNA density. Under these conditions, ≥90% of DNA from non-irradiated cells was recovered in the first gradient fractions corresponding to a buoyant density of ≥1.6. UVA irradiation caused a dose dependent increase in the fraction of DNA banding in the middle of the gradient at a density of around 1.4—intermediate between that of native DNA and protein (Figure 6A). This altered buoyant density is consistent with the covalent attachment of protein to DNA and a similar DNA density shift was observed in cells treated with formaldehyde, which is known to cause DNA–protein crosslinking (Figure 6A, top right insert).

The density shift of DNA from treated cells was reversed by extensive protease digestion of DNA samples before banding (proteinase K, 1 mg/ml final, 16 h at 50°C). This resulted in most of the radioactive 2-[14C]-thymidine labelled DNA being recovered close to the bottom of the gradient corresponding to a buoyant density of ≥1.6 (Figure 6B). In contrast to the effects of protease digestion, pre-treatment of the DNA samples with the reducing agents β-mercaptoethanol and DTT

(10 mM DTT, 1% β-mercaptoethanol, 50°C, 16 h) or with high temperature (15 min at 95°C; data not shown) before banding did not significantly affect DNA density (Figure 6B). This suggests that most of the protein–DNA attachment is not via disulphide linkages. Their thermal stability also distinguishes these photochemically induced complexes from those generated by formaldehyde treatment.

Control experiments confirmed that the DNA–protein crosslinks were formed within cells rather than during DNA extraction and processing when irradiated DNA and proteins are in intimate contact. When 6-TG-containing DNA was irradiated and mixed with CCRF-CEM cell proteins and banded, <10% was recovered at the position of reduced density (data not shown).

DNA in the vicinity of replication forks is particularly sensitive to breakage by 6-TG/UVA (12). To determine whether protein crosslinking exhibited a similar bias, we performed pulse-chase experiments. CCRF-CEM cells were allowed to incorporate 6-TG for 4 h. They were then irradiated with 50 kJ/m² UVA either immediately or following an additional 4 h growth in 6-TG free medium to allow replication forks to move away from the incorporated 6-TG. In both cases, ∼10% of the DNA exhibited reduced density (Supplementary Figure S4). Thus, crosslinking appears to be likely in any DNA regions containing 6-TG.

The UVA doses used to induce DNA–protein crosslinking are significantly less than one minimal erythema dose (9) and are therefore in the physiologically relevant range. In most experiments, cells containing an average DNA 6-TG substitution of around 1% 6-TG:G were used. This is more than an order of magnitude higher than the levels found in skin of patients treated with thiopurines (6). To assess whether patients' skin might be at risk for this type of DNA damage, we determined the lowest level of DNA 6-TG at which DNA–protein crosslinks were detectable in cultured cells. Crosslinking was detected in irradiated cells with DNA substitution of
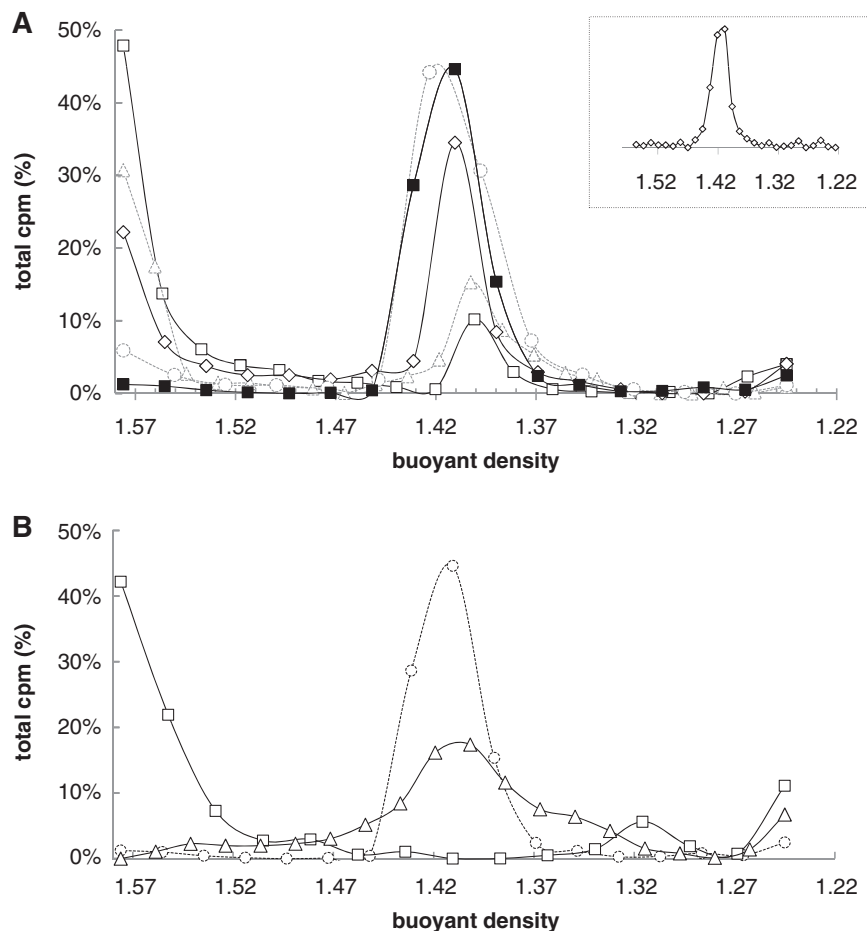
**Figure 6.** (**A**) Buoyant density of DNA from 6-TG/UVA-treated cells. 6-TG-treated CCRF-CEM cells, which had been labelled with 2-[$^{14}$C]-thymidine, were irradiated with UVA. Genomic DNA was extracted and the solution adjusted to a density of 1.4 with CsCl. Gradients were centrifuged to equilibrium and fractionated. Radioactivity in the fractions was measured by scintillation counting. DNA of normal density (1.70) is recovered in the first few fractions. (open square), No UVA; (open triangle), $5\,kJ/m^2$; (open diamond), $10\,kJ/m^2$; (open circle), $25\,kJ/m^2$; (filled square), $50\,kJ/m^2$. Insert: DNA banding from formaldehyde-treated cells. (**B**) Protease sensitivity of low-density DNA fractions. DNA from 6-TG/UVA ($50\,kJ/m^2$) treated CCRF-CEM cells was extracted and treated with Proteinase K (open square) or reducing agents (open triangle) or untreated (open circle) before banding on CsCl. Gradients were centrifuged and fractionated as above.

around 0.04% (range 0.034–0.058, $n = 2$), which is close to the levels of about 0.02% 6-TG:G in DNA of lymphocytes and skin of patients taking azathioprine (4–6). This suggests that photochemical DNA–protein crosslink formation may be a hazard for skin cells of patients on thiopurine therapy.

### DNA crosslinked DNA repair proteins

CsCl gradient fractions contain crosslinked material free from unmodified DNA or protein. Gradient fractions from 6-TG/UVA treated CCRF-CEM cells were applied to nitrocellulose membranes which were then probed for the presence of specific proteins. Figure 7 shows that two DNA repair proteins, MSH2 and the nucleotide excision repair (NER) factor XPA, the replication/repair factor PCNA and the replication factor MCM2, were all significantly represented in the crosslinked DNA fraction. There was no detectable DNA association of the largely cytoplasmic CASPASE 5.

## DISCUSSION

The skin of patients taking thiopurines contains DNA 6-TG and is selectively sensitive to UVA radiation (6,9). Since cutaneous photosensitivity reflects the formation of DNA lesions, it is important to understand what types of photochemical DNA damage may be produced by the interaction of DNA 6-TG and UVA.

In view of the reactivity of DNA 6-TG and its particular ability to form addition products with low-molecular weight thiol compounds (10), we examined crosslinking of proteins to DNA 6-TG. Photochemical adduction of purified proteins to DNA containing 6-TG has previously been demonstrated (20,21). In our *in vitro* experiments, we found that $G^{SO3}$, the oxidized form of 6-TG, was a likely intermediate in peptide crosslinking. This may, in part, reflect the ability of $SO_3$ to serve as a good leaving group in nucleophilic substitution reactions (10). Most of the products were susceptible to reducing treatments—consistent with the formation of disulphide bridges between the cysteine thiol and 6-TG. A minority

Fraction density

High  Med  Low
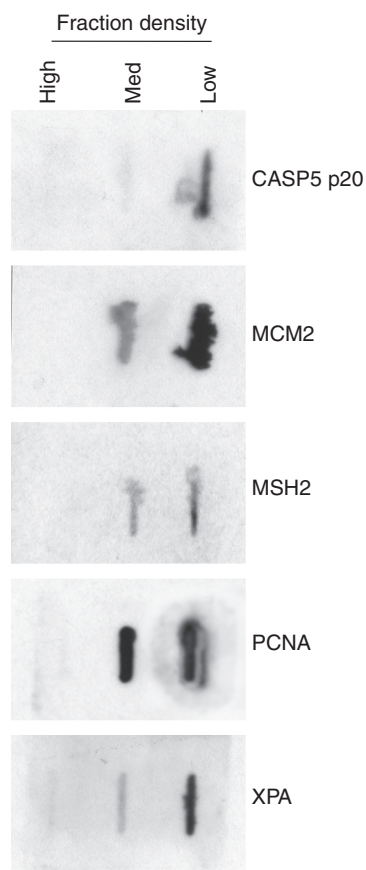


**Figure 7.** Crosslinked DNA repair and replication proteins. Extracts of CCRF-CEM cells treated with 6-TG ($0.6 \mu M$, 48 h) and UVA ($20 \, kJ/m^2$) were extracted and banded on CsCl. Fractions corresponding to high ($\geq 1.7$), medium (ca 1.4) or low ($\leq 1.30$) density were pooled, desalted and concentrated. Approximately $500 \, \mu l$ of a $0.35 \, A_{260}$ solution of each fraction was applied to a hybond N nitrocellulose membrane that was probed with the antibodies indicated.

involved free amino groups of the polypeptide and crosslinking was reduced when these were blocked by acetylation.

DNA–protein crosslinks from UVA-irradiated cells were largely refractory to reducing treatments. This suggests that, unlike the *in vitro* crosslinks, disulphide protein–DNA bridges are not highly represented among these *in vivo* products. This may simply reflect the relative concentrations of –SH and –$NH_2$ groups in the *in vitro* and *in vivo* experiments. Although primary amino groups of this type are less nucleophilic than thiols, they are much more abundant *in vivo* and the amino acids with a free amino group (R, N, Q, K) represent about 20% of all amino acids in human proteins. In contrast, the more hydrophobic cysteine comprises only 1.7% of the total (source: UniProtKB/Swiss-Prot protein knowledgebase, release 2011-01). The hydrophilic nature of amino groups also means that they are frequently exposed on the protein surface. For these reasons, we consider it possible that these N-bonded proteins comprise a significant fraction of the DNA 6-TG-protein crosslinks formed in UVA-irradiated cells. We noted significant differences

in the kinetics of crosslinking *in vivo* and *in vitro*, however. This may partially reflect the structural arrangement of the crosslinked partners. The reaction of the oligonucleotide $G^{SO3}$ with the oligopeptide –SH or –$NH_2$ groups occurs in relatively dilute solution. In the cell, the close proximity of DNA associated proteins to any $G^{SO3}$ that is formed may significantly accelerate crosslinking. An alternative explanation invokes a different photochemistry for DNA 6-TG. The formation of $G^{SO3}$ is via singlet oxygen and Type II photosensitization. It is possible that 6-TG can also act as a Type I photosensitizer and the rapid formation of DNA–protein crosslinks *in vivo* is consistent with a free radical intermediate that can react only with proteins in extremely close proximity. At present, we cannot distinguish between these possibilities.

We previously demonstrated photochemical damage to proteins in the form of inter-subunit crosslinks in the DNA replication/repair protein PCNA (8). The vulnerability of PCNA was confirmed in this study by a 2-D DIGE analysis of nuclear proteins from 6-TG/ UVA-treated cells, which revealed consistent alterations to PCNA and to a number of other DNA repair/replication related proteins, including MSH2 and MSH6. UVA irradiation was associated with a measurable reduction in overall recovery of nuclear MSH2. This suggests that sequestration of this essential mismatch repair protein might reduce repair efficiency. Isopycnic density gradient analysis revealed the extensive formation of DNA–protein crosslinks that was dependent on both 6-TG and UVA. To our knowledge, this is the first demonstration that DNA 6-TG mediates photochemical DNA–protein adduction in intact cells. Several lines of evidence indicate that crosslinking is extensive. Even at low doses of UVA, most of the 6-TG DNA fragments sheared to an average size of around 15 kb, become associated with protein. Assuming a Poisson distribution, for 80% of DNA fragments to be density shifted, (corresponding to $10 \, kJ/m^2$ UVA in Figure 6A), there will be, on average, approximately one adducted protein for every 6 kb of DNA. Comparison of DNA 6-TG photoproduct yields *in vitro* and in irradiated cells also indicates that DNA–protein crosslinks are abundant. Following UVA irradiation *in vitro* the known oxidation products, $G^{SO2}$ and $G^{SO3}$, account for around 90% of photochemically destroyed DNA 6-TG (10). In UVA-irradiated cells, however, up to 20–40% of DNA 6-TG is converted to as yet unidentified photoproducts (22). At 1% DNA substitution by 6-TG, a protein adduct would occur every 10 kb of DNA even if DNA–protein crosslinks comprise only 10% of these unidentified photoproducts. Finally, we note that crosslinks were detectable following exposure of cells to physiological UVA doses and at DNA substitution levels approaching those found in the skin of patients taking azathioprine. We conclude that these lesions may contribute significantly to the biological effects of 6-TG/UVA.

The resolution afforded by gradients allowed us to identify some of the proteins that are crosslinked to a significant extent. As expected, PCNA and MSH2, which had previously been identified as likely targets, were present in the crosslinked DNA fraction whereas

CASPASE 5, regarded to have an overwhelmingly cytoplasmic distribution, was not. This analysis was not exhaustive but nevertheless provides clear evidence that DNA-related nuclear proteins are at risk of covalent attachment to DNA. The approach has the potential to address the unresolved question of DNA–protein crosslink repair in human cells. There are suggestions that smaller adducts can be removed by a mechanism that is partially dependent on NER(23,24) In our experiments, the overall removal of 6-TG-mediated crosslinks was, at best, extremely slow and the fraction of density shifted DNA did not change significantly up to 24-h post irradiation (data not shown). These observations are consistent with suggestions that large DNA–protein adducts are not efficiently repaired by NER. From a chemical point of view, the protein–DNA bonds are robust and are unaffected by extended treatment with heat, salts and reducing agents. Indeed, it seems likely that there is no effective method of removing these lesions and the cells need to process the aftermath of their interaction with replication. Consistent with this view, homologous recombination plays a critical role in the tolerance of crosslinked proteins (25,26). The more refined analysis that can be applied to the individual crosslinked proteins in the gradient fraction will permit analysis of the fate of individual crosslinked species.

In summary, we have demonstrated numerous alterations to the nuclear proteins of UVA-irradiated cells containing DNA 6-TG. These changes include a rapid and efficient formation of stable covalent DNA–protein crosslinks. It seems likely that DNA–protein crosslinking will influence DNA repair—either by steric hindrance preventing binding and/or translocation of repair proteins or by their physical sequestration. We have provided the first evidence for the latter possibility. Our findings indicate that, overall DNA–protein crosslinks are not efficiently repaired but the analysis outlined here will permit a more detailed investigation of the fate of individual crosslinked protein species. Any significant interference with DNA repair might, by reducing the efficiency of excision of pro-mutagenic UVB-induced DNA lesions, increase the potential mutagenicity of sunlight in skin of long-term immunosuppressed patients and thereby contribute to their increased skin cancer risk.

## SUPPLEMENTARY DATA

Supplementary Data are available at NAR Online.

## FUNDING

*Conflict of interest statement*. None declared.

## REFERENCES

1. Grosse,Y., Baan,R., Straif,K., Secretan,B., El Ghissassi,F., Bouvard,V., Benbrahim-Tallaa,L., Guha,N., Galichet,L. and Cogliano,V. (2009) A review of human carcinogens-Part A: pharmaceuticals. *Lancet Oncol.*, **10**, 13–14.
2. Euvrard,S., Kanitakis,J. and Claudy,A. (2003) Skin cancers after organ transplantation. *N. Engl. J. Med.*, **348**, 1681–1691.
3. Penn,I. (1994) The problem of cancer in organ transplant recipients: an overview. *Transplant Sci.*, **4**, 23–32.
4. Warren,D.J., Andersen,A. and Slordal,L. (1995) Quantitation of 6-thioguanine residues in peripheral blood leukocyte DNA obtained from patients receiving 6-mercaptopurine-based maintenance therapy. *Cancer Res.*, **55**, 1670–1674.
5. Cuffari,C., Li,D.Y., Mahoney,J., Barnes,Y. and Bayless,T.M. (2004) Peripheral blood mononuclear cell DNA 6-thioguanine metabolite levels correlate with decreased interferon-gamma production in patients with Crohn's disease on AZA therapy. *Dig. Dis. Sci.*, **49**, 133–137.
6. O'Donovan,P., Perrett,C.M., Zhang,X., Montaner,B., Xu,Y.Z., Harwood,C.A., McGregor,J.M., Walker,S.L., Hanaoka,F. and Karran,P. (2005) Azathioprine and UVA light generate mutagenic oxidative DNA damage. *Science*, **309**, 1871–1874.
7. Zhang,X., Jeffs,G., Ren,X., O'Donovan,P., Montaner,B., Perrett,C.M., Karran,P. and Xu,Y.Z. (2007) Novel DNA lesions generated by the interaction between therapeutic thiopurines and UVA light. *DNA Repair*, **6**, 344–354.
8. Montaner,B., O'Donovan,P., Reelfs,O., Perrett,C.M., Zhang,X., Xu,Y.Z., Ren,X., Macpherson,P., Frith,D. and Karran,P. (2007) Reactive oxygen-mediated damage to a human DNA replication and repair protein. *EMBO Rep.*, **8**, 1074–1079.
9. Perrett,C.M., Walker,S.L., O'Donovan,P., Warwick,J., Harwood,C.A., Karran,P. and McGregor,J.M. (2008) Azathioprine treatment photosensitizes human skin to ultraviolet A radiation. *Br. J. Dermatol.*, **159**, 198–204.
10. Ren,X., Li,F., Jeffs,G., Zhang,X., Xu,Y.Z. and Karran,P. (2010) Guanine sulphinate is a major stable product of photochemical oxidation of DNA 6-thioguanine by UVA irradiation. *Nucleic Acids Res.*, **38**, 1832–1840.
11. Brem,R., Li,F. and Karran,P. (2009) Reactive oxygen species generated by thiopurine/UVA cause irreparable transcription-blocking DNA lesions. *Nucleic Acids Res.*, **37**, 1951–1961.
12. Brem,R., Li,F., Montaner,B., Reelfs,O. and Karran,P. (2010) DNA breakage and cell cycle checkpoint abrogation induced by a therapeutic thiopurine and UVA radiation. *Oncogene*, **29**, 3953–3963.
13. Au,V. and Madison,S.A. (2000) Effects of singlet oxygen on the extracellular matrix protein collagen: oxidation of the collagen crosslink histidinohydroxylysinonorleucine and histidine. *Arch. Biochem. Biophys.*, **384**, 133–142.
14. Davies,M.J. (2004) Reactive species formed on proteins exposed to singlet oxygen. *Photochem. Photobiol. Sci.*, **3**, 17–25.
15. Cramer,P., Bushnell,D.A. and Kornberg,R.D. (2001) Structural basis of transcription: RNA polymerase II at 2.8 angstrom resolution. *Science*, **292**, 1863–1876.
16. Gnatt,A.L., Cramer,P., Fu,J., Bushnell,D.A. and Kornberg,R.D. (2001) Structural basis of transcription: an RNA polymerase II elongation complex at 3.3 A resolution. *Science*, **292**, 1876–1882.
17. Warren,J.J., Pohlhaus,T.J., Changela,A., Iyer,R.R., Modrich,P.L. and Beese,L.S. (2007) Structure of the human MutSalpha DNA lesion recognition complex. *Mol. Cell*, **26**, 579–592.
18. Taverna,P., Liu,L., Hanson,A.J., Monks,A. and Gerson,S.L. (2000) Characterization of MLH1 and MSH2 DNA mismatch repair proteins in cell lines of the NCI anticancer drug screen. *Cancer Chemother. Pharmacol.*, **46**, 507–516.
19. Maniatis,T., Sambrook,J. and Fritsch,E. (1982) *Molecular Cloning: A Laboratory Manual*. Cold Spring Harbor Press, New York.
20. Cahill,M.A., Nordheim,A. and Xu,Y.Z. (1996) Crosslinking of SRF to the c-fos SRE CArG box guanines using photo-active thioguanine oligodeoxynucleotides. *Biochem. Biophys. Res. Commun.*, **229**, 170–175.
21. Favre,A., Saintome,C., Fourrey,J.L., Clivio,P. and Laugaa,P. (1998) Thionucleobases as intrinsic photoaffinity probes of nucleic acid structure and nucleic acid-protein interactions. *J. Photochem. Photobiol. B.*, **42**, 109–124.

22. Li,F. (2010) DNA damage and UVA-induced oxidation of 6-thioguanine. *PhD Thesis*. University of London, London.

23. Nakano,T., Morishita,S., Katafuchi,A., Matsubara,M., Horikawa,Y., Terato,H., Salem,A.M., Izumi,S., Pack,S.P., Makino,K. *et al.* (2007) Nucleotide excision repair and homologous recombination systems commit differentially to the repair of DNA-protein crosslinks. *Mol. Cell*, **28**, 147–158.

24. Reardon,J.T. and Sancar,A. (2006) Repair of DNA-polypeptide crosslinks by human excision nuclease. *Proc. Natl Acad. Sci. USA*, **103**, 4056–4061.

25. Nakano,T., Katafuchi,A., Matsubara,M., Terato,H., Tsuboi,T., Masuda,T., Tatsumoto,T., Pack,S.P., Makino,K., Croteau,D.L. *et al.* (2009) Homologous recombination but not nucleotide excision repair plays a pivotal role in tolerance of DNA-protein cross-links in mammalian cells. *J. Biol. Chem.*, **284**, 27065–27076.

26. Ridpath,J.R., Nakamura,A., Tano,K., Luke,A.M., Sonoda,E., Arakawa,H., Buerstedde,J.M., Gillespie,D.A., Sale,J.E., Yamazoe,M. *et al.* (2007) Cells deficient in the FANC/BRCA pathway are hypersensitive to plasma levels of formaldehyde. *Cancer Res.*, **67**, 11117–11122.